Flow and Compressive Strength of Alkali-Activated Mortars

Keun-Hyeok Yang[a], Jin-Kyu Song[b], Kang-Seok Lee[c], and Ashraf F. Ashour[d]

[a] *Corresponding author, Department of Architectural Engineering, Mokpo National University, Mokpo, Jeonnam, South Korea, Tel: +82 (0)61 450 2456, Fax: +82 (0)61 450 6454, E-mail: yangkh@mokpo.ac.kr*

[b] *Department of Architectural Engineering, Chonnam National University, Jeonnam, South Korea.*

[c] *Department of Architectural Engineering, Chonnam National University, Jeonnam, South Korea.*

[d] *EDT 1, School of Engineering, Design and Technology, University of Bradford, Bradford, BD7 1DP, UK.*

Biography: K. H. Yang is an assistant professor at Mokpo National University, Korea. He received his MSc and PhD degrees from Chungang University, Korea. He was a visiting research fellow at the University of Bradford, UK. His research interests include ductility, recycling, strengthening, plasticity and shear of reinforced concrete structures including alkali-activated concrete.

J. K. Song is an associate professor at Chonnam National University, Gwangju, Korea. He received his BS, MS and PhD degrees from Seoul National University, Seoul, Korea. He chairs Biohousing Research Institute supported by the Korea Research Foundation Grant. His research interests include alkali-activated concrete, shear and moment capacity evaluations of slab-column connections of concrete structures, and seismic design of concrete structures.

K. S. Lee is an assistant professor at Chonnam National University, Gwangju, Korea. He received his MS and PhD degrees from the University of Tokyo, Japan. He was a guest researcher at the Building and Fire Research Laboratory, National Institute of Standards and Technology, Gaithersburg, Maryland. His research interests include seismic capacity evaluation and rehabilitation of concrete structures, alkali-activated concrete, and optimal structural design of concrete structures.

A. F. Ashour is a senior lecturer at the University of Bradford, UK. He obtained his BSc and MSc degrees from Mansoura University, Egypt and his PhD from Cambridge University, UK. His research interests include shear, plasticity and optimization of reinforced concrete and masonry structures.

ABSTRACT

Test results of thirty six ground granulated blast-furnace slag (GGBS)-based mortars and eighteen fly ash (FA)-based mortars activated by sodium silicate and/or sodium hydroxide powders are presented. The main variables investigated were the mixing ratio of sodium oxide (Na_2O) of the activators to source materials, water-to-binder ratio, and fine aggregate-to-binder ratio. Test results showed that GGBS based alkali-activated (AA) mortars exhibited much higher compressive strength but slightly less flow than FA based AA mortars for the same mixing condition.

Feed-forward neural networks and simplified equations developed from nonlinear multiple regression analysis were proposed to evaluate the initial flow and 28-day compressive strength of AA mortars. The training and testing of neural networks, and calibration of the simplified equations were achieved using a comprehensive database of 82 test results of mortars activated by sodium silicate and sodium hydroxide powders. Compressive strength development of GGBS-based alkali-activated mortars was also estimated using the formula specified in ACI 209 calibrated against the collected database. Predictions obtained from the trained neural network or developed simplified equations were in good agreement with test results, though early strength of GGBS-based alkali-activated mortars was slightly overestimated by the proposed simplified equations.

Keywords: alkali-activated mortar, fly ash, ground granulated blast furnace slag, neural network, regression analysis.

INTRODUCTION

It has been generally recognized[1-5] that fly ash (FA) and ground granulated blast-furnace slag (GGBS)-based alkali-activated (AA) binders are practically useful construction materials owing to their sound environmental performance such as recycling of by-product materials, low carbon dioxide emissions and low energy consumption. In addition, AA concrete has been known to have many beneficial properties compared with ordinary Portland cement (OPC) concrete such as rapid high strength development, good durability and high resistance to chemical attack[1]. As a result, the application of AA mortar or concrete has gradually grown to a large proportion in the construction industry.

Extensive reviews[2-3, 6-10] on AA binders clearly showed that calcined materials with abundant silicon oxide (SiO_2), aluminum oxide (Al_2O_3), and/or calcium oxide (CaO) are suitable source materials as the mechanism of alkali activation process involves a chemical reaction between various alumino-silicate oxides with silicate, and/or the formation of silica-rich calcium silicate hydrates gel (CSH gel). It is also known[7, 8] that alkali hydroxide (ROH), non-silicic salts of weak acids (R_2CO_3, R_2S, RF), or silicic salts of $R_2O{\cdot}(n)SiO_2$ type can be used as effective activators, where R indicates an alkali metal ion such as Na, K or Li. Various important parameters affecting the activation mechanism of AA mortar are well evaluated as summarized in different review papers[2-3, 8-10]. Although, numerous investigations[8, 10] are published on the optimum mix design of mortar or concrete activated by alkaline solutions, very few test data[11] on concrete activated by powder type activators are available. However, mortar and concrete in construction industry are

generally manufactured from powder-type binders. Compared with powder-type activators, solution-type activators are more effective for high-strength concrete, but require more caution to handle safely outside the laboratory environment[12]. Therefore, it is necessary to carry out more experimental investigations on mortar or concrete activated by powder-type activators to improve the practical application of AA binders.

Although, there have been many theoretical investigations[13] to evaluate the workability and strength of OPC mortar or concrete, they are not applicable to assess the properties of AA mortars as the hydration mechanism of both pastes are completely different. In addition, it is difficult to control the strength development of AA mortars owing to the inconsistent interaction of numerous influencing factors as pointed out by Wang et al[1]. The current investigation presents test results of GGBS and FA based AA mortars of different mixing ratios of sodium oxide (Na_2O) of the activators to source materials by weight, water to binder, and fine aggregate to binder. Multi-layered feed-forward neural networks were also developed to model the nonlinear interaction between initial flow and compressive strength of AA mortars, and different influencing parameters.

RESEARCH SIGNIFICANCE

Utilization of AA mortars using powder-type activators would contribute to the solution of recycling of by-product materials, and reduction of carbon dioxide emission and energy consumption owing to OPC production. However, test data on AA activated mortar properties such as flow and compressive strength are limited. The experimental and analytical results of the present

study can be practically applied for reliable mix design of mortars activated by sodium silicate and sodium hydroxide powders.

EXPERIMENTAL PROGRAMME

Mix design

AA mortars studied were classified into three groups as given in Table1: group I and group II for GGBS and FA based mortars, respectively, activated by combined sodium silicate and sodium hydroxide powders, and group III for GGBS-based mortar activated by sodium silicate only. Main variables investigated in each group were the amount of added alkaline activators, water-to-binder (W/B) ratio, and fine aggregate-to-binder (S/B) ratio, where W and S is the weight of water and fine aggregate, respectively, and B indicates the total weight of the binder and alkaline activator. The amount of alkaline activators added was controlled by Na_2O of the activator to source material (SM) ratio by weight. The Na_2O/SM ratios selected in all groups were 0.038 and 0.089 to produce low and medium strength GGBS-based AA mortars, respectively, as proposed by Yang et al[14]. Sodium hydroxide powder was also added in groups Ⅰ and II to control the molar ratio (SiO_2/Na_2O) of the sodium silicate at the same Na_2O/SM ratio. As a result, the SiO_2/Na_2O ratio of added activators was 0.75 in groups I and II, and 0.9 in group III. The W/B ratio varied from 0.3 to 0.6 in mortars mixed with S/B ratio of 3.0. For W/B ratio = 0.5, S/B ratio also ranged from 0 to 3.5 as presented in Table 1.

Materials

The Blaine fineness and specific gravity of FA were 3388 cm^2/g (525 $in.^2/g$) and 2.2, respectively, and those of GGBS were 4204 cm^2/g (652 $in.^2/g$) and 2.9, respectively. The chemical compositions of GGBS and FA obtained from x-ray fluorescence (XRF) analysis are given in Table 2. The X-ray powder diffraction pattern recorded for source materials used is also shown in Fig. 1. The FA used had a low calcium oxide (CaO) but was rich in both silicon and alumina as the silicon oxide (SiO_2)-to-aluminum oxide (Al_2O_3) ratio by mass is 1.91 which belongs to class F according to the American Society for Testing and Materials standards[15]. In addition, the most abundant phase in fly ash is glass including quartz and mullite as shown in Fig. 1. On the other hand, GGBS was mainly composed of calcium, silicon, alumina and magnesium oxides. Three characteristic peaks corresponding to dicalcium silicate and spinel appeared on XRD patterns for GGBS. Sodium silicate powder and sodium hydroxide powder, commercially available in South Korea, were used as activators. The sodium silicate powder used as the main activator in all mortars composed of 50.2 % sodium oxide (Na_2O) and 45 % silicon oxide (SiO_2), producing a molar ratio of 0.9. The maximum particle size of sodium silicate was 0.5 mm (0.02 in.). The sodium hydroxide powder with a maximum particle size of 0.5 mm (0.02 in.) was also employed as an auxiliary activator in groups I and II. Locally available sand with maximum size of 5 mm (0.2 in.) was used as the fine aggregate in saturated surface-dry condition. The specific gravity and grading of the sand were 2.54 and 2.97, respectively.

Casting, curing, and testing

The source material, activator, and fine aggregate were dry-mixed in a mixer pan for 30 seconds, and water was then added and mixed for another 30 seconds. After initial flow testing, each mix mortar was poured in steel moulds of dimensions 50×50×50 mm (1.97×1.97×1.97 in.) to measure the compressive strength. Immediately after casting, all specimens were cured at room temperature having constant relative humidity of 70 ± 5% until tested at a specified age. All steel moulds for GGBS-based AA mortars were removed at an age of one day, while those for FA-based AA mortars were removed after three days of casting as they required more setting time.

The test procedure of initial flow and compressive strength was carried out according to American Society for Testing and Materials standards[15]. Initial flow of mortar was measured using a cone-shaped mould having a height of 50 mm (1.97 in.), a bottom diameter of 100 mm (3.94 in.) and a top diameter of 70 mm (2.76 in.). Immediately after filling the mould that is mounted rigidly on the flow table, the cone is slowly lifted, and then the flow table was jolted 15 times in a period of 60 seconds. The mortar consequently spreads out and the maximum spread parallel to the two edges of the table was recorded. Compressive strength development of mortar was monitored by testing three mortar cubes at 1, 3, 7, 28, 56 and 91 days using a 500 kN (112 kip) capacity universal testing machine.

TEST RESULTS AND DISCUSSION

Initial flow

The initial flow F_i of AA mortars was significantly influenced by W/B and S/B ratios as shown in Fig. 2 and Table 1. The flow of AA mortars tested proportionally increased with the increase of W/B ratio and decreased with the increase of S/B ratio. On the other hand, the initial flow of AA mortars with Na_2O/SM ratio of 0.089 was slightly lower than that of AA mortars with Na_2O/SM ratio of 0.038 at the same W/B and S/B ratios. A slightly higher flow also occurred in FA-based AA mortars than GGBS-based AA mortars for the same mixing condition. Although, there is no consensus view on the setting mechanism of AA mortars, the absence of tricalcium silicate ($3CaO{\cdot}SiO_2$) and tricalcium aluminate ($3CaO{\cdot}Al_2O_3$) in source material would cause quick setting of mortar[1]. In addition, higher fineness of source material is more reactive and requires more water for hydration, resulting in quicker setting of mortar[2]. On the other hand, a relatively low curing temperature of FA-based AA mortar leads to a slower reaction as stable alkali reaction process of FA requires a higher temperature to accelerate the hydrothermal synthesis reaction. The spherical shape of FA particles also helps in producing higher initial flow[8] than non-spherical slag.

Compressive strength at 28 days

The influence of W/B, S/B, and Na_2O/SM ratios on the 28-day compressive strength $\left(f_c^{'}\right)_{28}$ of AA mortars was dependent on the type of source material as given in Table 1. No meaningful compressive strength $\left(f_c^{'}\right)_{28}$ developed in FA-based AA mortars tested. However, much higher

$\left(f_c^{'}\right)_{28}$ exhibited by GGBS-based AA mortars. From the energy-dispersive X-ray (EDX) analysis combined with scanning electron microscope (SEM) image, Yang and Song[16] showed that very few hydration products were detected in FA-based AA mortars cured under room temperature, which would be the main cause of the poor compressive strength of the FA-based AA mortars. On the other hand, the effect of Na_2O/SM ratio on $\left(f_c^{'}\right)_{28}$ was clearly shown in GGBS-based AA mortars as increasing Na_2O/SM ratio from 0.038 to 0.089 produced an increase in $\left(f_c^{'}\right)_{28}$ by an average of 220% at the same W/B and S/B ratios. The 28-day compressive strength $\left(f_c^{'}\right)_{28}$ of GGBS-based mortars activated by the combination of sodium silicate and sodium hydroxide was generally lower than that of GGBS-based mortars activated by sodium silicate only for the same value of Na_2O/SM ratio.

The influence of W/B and S/B ratios on the 28-day compressive strength $\left(f_c^{'}\right)_{28}$ of AA mortars studied is shown in Fig. 3. The 28-day compressive strength $\left(f_c^{'}\right)_{28}$ of AA mortars tested commonly decreased with the increase of W/B ratio, similar to the trend observed in OPC concrete[13]. The decreasing rate was more prominent in AA mortars with Na_2O/SM ratio of 0.089 than 0.038. Although, there is no consensus view on the role of Na^+ cation in the hydration process of GGBS-based paste activated by sodium silicate or sodium hydroxide, it is generally agreed[1, 6] that Na^+ ion plays a catalytic role involving interchange with Ca^{2+} cations. As a result, the negatively charged surface of C-S-H gel would tightly sorb some Na^+ cations and Na-substituted C-S-H gel can be presented[1]. On the other hand, Na^+ cation would help in balancing and maintaining OH^- anions; thus some structurally bounded Na^+ cations are removed from the C-S-H gel[1]. In

addition, the extent of dissolution of GGBS particles increases with the increase of the pH of the solution present. However, when W/B ratio is too high, the increase of the pH is not so high and consequently the strength drops. Therefore, higher Na_2O/SM ratio would result in higher compressive strength of AA mortars, but cause a sharp decrease of the compressive strength with the increase of W/B ratio as shown in Fig. 3. On the other hand, the measured $\left(f_c^{'}\right)_{28}$ of GGBS-based AA mortars increased with the increase of S/B ratio up to a value of S/B = 2.5 regardless of Na_2O/SM ratio, beyond which it dramatically decreased. In general, compressive strength of OPC mortar increases with the increase of S/B ratio up to a value of S/B = 3.0~3.5[13]. Therefore, the threshold of S/B of AA mortars would be slightly lower than that of OPC mortar, though further investigations would be required to confirm this conclusion.

Compressive strength development

Yang and Song[14, 16] showed that the compressive strength development of GGBS-based AA mortar according to age could be modeled using the formula recommended by ACI 209[17] as follows:

$$f_c^{'}(t) = \frac{t}{A_1 + B_1 t}\left(f_c^{'}\right)_{28} \quad (1)$$

where $f_c^{'}(t)$ is the compressive strength at age t (in days). The parameters A_1 and B_1 in Eq. (1) representing a parabolic function generally relate to the development of strength at an early age and a long-term age, respectively; lower values of A_1 and B_1 correspond to higher compressive strength at early age and long-term age, respectively. On the other hand, the compressive strength of FA-based AA mortars tested linearly developed with age (see Table 1) and therefore, would not be reasonably modelled using Eq. (1).

Fig. 4 shows the effect of W/B and S/B ratios on the parameters A_1 and B_1 of Eq. (1). The parameter A_1 increased with the increase of W/B ratio and increase of Na_2O/SM ratio. In addition, the parameter A_1 increased with the increase of S/B ratio until S/B ratio of 2.5, similar to the trend observed in $\left(f_c^{'}\right)_{28}$ given in Fig. 3 (b). Considering that A_1 for OPC concrete or mortar is commonly assumed to be 4.0[17], this parameter for GGBS-based AA mortars would be lower as GGBS-based AA mortars gain higher strength at early age. The parameter B_1 obtained for GGBS-based AA mortar tested was less influenced by W/B and Na_2O/SM ratios but nearly independent on S/B ratio. A slightly lower B_1 was obtained for GGBS-based AA mortars with a higher W/B ratio and a lower Na_2O/SM ratio. This indicates that the long-term rate of compressive strength development of GGBS-based AA mortars increases with the increase of W/B ratio and the decrease of Na_2O/SM ratio.

NEURAL NETWORK MODELLING

Neural network architecture

Artificial neural networks (NNs) are a useful tool to reasonably predict performance of concrete if many reliable test data are available as pointed out by Kaveh and Khalegi[18]. A typical multi-layered feed-forward NN without input delay is composed of an input layer, one or more hidden layers and an output layer as shown in Fig. 5, where **P** indicates the input vector, **IW** and **LW** give the weight matrices for input and hidden layers, respectively, **b** represents the bias vector, and **n** is the net input passed to the transfer function ***f*** to produce the neuron's output vector ***y***. Back-propagation is

generally known to be the most powerful and widely used for NN training[19]. Weights and biases are adjusted using a number of training inputs and the corresponding target values. The network error is then back propagated from the output layer to the input layer to update the network weights and biases. The adjusting process of neuron weights and biases is carried out until the network error arrives at a specific level of accuracy.

To control overfittings in the training process, early stopping technique is generally recognized to be one of the most effective methods[19]. In this technique, the available data are divided into three subsets; training, validation and test subsets. The training set is used for computing the gradient and updating the network weights and biases to diminish the training error. When the error on the validation set increases for a specified number of iterations, the training is stopped, and then the network weights and biases at the minimum validation error are returned. The test set error is not used during the training, but it is used for verification of the NNs and comparison of different models.

The present tests showed that Na_2O/SM ratio is one of the main parameter affecting the compressive strength of GGBS-based mortars activated by sodium silicate and sodium hydroxide as also concluded by Wang et al.[6]. However, the Na_2O/SM ratio cannot reflect the effect of the molar Si-to-Al ratio and calcium content in the source material on the mechanical strength of alkali-activated paste. Yang et al.[14] proposed an alkali quality coefficient Q_A as an effective index to evaluate the workability and compressive strength of AA mortars using sodium silicate and sodium hydroxide powders:

$$Q_A = \left(\frac{Na_2O}{(SiO_2)^2} \cdot Al_2O_3 \cdot CaO \right) \Big/ B \quad \text{(by weight)} \tag{2}$$

Q_A combines the concentration of the activator and main composition of source materials in alkali-activated binder using sodium silicate and sodium hydroxide powders. Therefore, two NNs, namely Networks A and B, with different input neurons were built and compared. For neural network A, six neurons representing the type of source material and alkaline activators, Blaine fineness S_A of source materials, Na_2O/SM ratio, W/B ratio, and S/B ratio were identified in the input layer as shown in Fig. 5 (a), whereas four neurons having Q_A, S_A, W/B ratio, and S/B ratio were provided in the input layer of neural network B as shown in Fig. 5 (b). In addition, for each network, two different NNs were built: one to determine the initial flow F_i and the other to estimate the 28-day compressive strength $(f_c')_{28}$ of AA mortars.

Experimental Database

82 test results of AA mortars were compiled from current tests and Yang et al.[14,16] and rearranged according to the designed input variables. The number of FA-based and GGBS-based specimens in the database is 6 and 24, respectively, for mortars activated by sodium silicate only, and 24 and 28, respectively, for mortars activated by the combination of sodium silicate and sodium hydroxide powders. To improve the performance of the developed NNs, the Blaine fineness S_A of source materials in input layer was normalized by a reference Blaine fineness S_{A0} of 4000 cm^2/g (620 $in.^2/g$).

Table 3 gives the range of input data in training, validation and test subsets used to develop the

NNs. Training, validation and test subsets had 50%, 25%, and 25% of all specimens in the database, respectively. The input data in each subset were selected throughout the database so that the range of input in the training subset would cover the entire distribution of database and input in the validation subset would stand for all points in the training subset as shown in Table 3.

Building of Neural Network

The NN toolbox available in MATLAB Version 6.0[19], which can be conveniently implemented to model large-scale problems, was used for building of the current NN model. In the hidden and output layers of the developed NNs, tan-sigmoid and linear transform functions, respectively, were employed for a training process. As upper and lower bounds of tan-sigmoid function output are +1 and -1, respectively, input and target in database were normalized using Eq. (3) below so that they fall in the interval [-1, 1].

$$(p_i)_n = \frac{2(p_i - (p)_{\min})}{(p)_{\max} - (p)_{\min}} - 1 \tag{3}$$

where $(p_i)_n$ and p_i = normalized and original values of data set, and $(p)_{\min}$ and $(p)_{\max}$ = minimum and maximum values of the parameter under normalization, respectively. Also, after training and simulation, outputs having the same units as the original database can be obtained by rearranging Eq. (3) as follows:

$$p_i = \frac{[(p_i)_n + 1][(p)_{\max} - (p)_{\min}]}{2} + (p)_{\min} \tag{4}$$

The number of hidden layers and neurons in each hidden layer has generally influence on the overfittings and predictions in training and outputs of NNs. Hence, trial and error approach was

carried out to find an adequate number of hidden layers and neurons in each hidden layer as given in Table 4. In addition, NN performance is significantly dependent on initial conditions[15] such as initial weights and biases, back-propagation algorithms, and learning rate. In NNs presented in Table 4, the following features were applied:

- initial weights and biases were randomly assigned by MATLAB Version 6.0;
- resilient back-propagation algorithm was selected;
- learning rate and momentum factor were assigned 0.4 and 0.2, respectively, and
- mean square error (MSE) was used to monitor the network performance, where MSE $= \frac{1}{N}\sum_{i=1}^{N}(T_i - A_i)^2$, N = total number of training points, T_i and A_i = target and actual outputs of specimen i, respectively.

The training process was also stopped when one of the following conditions was satisfied:

- the performance was minimized to the required target (MSE < 0.0001); or
- the validation set error starts to rise for a number of iterations.

Statistical comparisons between outputs and targets for total points of database according to the number of hidden layers and neurons in each hidden layer are presented in Table 4. Each statistical value in Table 4 is the average of 30 different trials where different random initial weights and biases are employed. Although the mean γ_m and standard deviation γ_s of the ratios between experiments and predictions by different NN architectures were close to each other, 6×12×6×1 and 4×8×4×1 NNs of which are the most successful for networks A and B, respectively. In particular,

the NNs with 4-layer do not show any overfitting during training. In addition, predictions obtained from network B were in better agreement with test results compared with network A, indicating that Q_A can be employed as an important parameter for evaluating the properties of mortars activated by sodium silicate and sodium hydroxide powders. Therefore, the 4×8×4×1 network B shown in Fig. 5 (b) was finally selected to predict F_i and $\left(f_c^{'}\right)_{28}$ of mortars activated by sodium silicate and sodium hydroxide powders. It should be noted that the two selected 4×8×4×1 networks for the prediction of F_i and $\left(f_c^{'}\right)_{28}$ of AA mortars have different initial weight matrices and bias vectors.

NONLINEAR MULTIPLE REGRESSION ANALYSIS

Nonlinear multiple regression (NLMR) analysis of the database compiled above was also carried out using SPSS software[20] to predict F_i and $\left(f_c^{'}\right)_{28}$ of AA mortars, and the two parameters A_1 and B_1 required for Eq. (1). In establishing the basic models, Q_A, S_A, W/B ratio and S/B ratio were considered as the main variables influencing the properties of AA mortars, as concluded from the NNs developed above. Each variable considered was combined and tuned repeatedly by trial and error approach using SPSS software until a relatively higher correlation coefficient was obtained. As pointed out by Wang et al.[1] and Pacheco-Torgal et al.[2], flow and compressive strength of AA mortars would much fluctuate even owing to periphery conditions such as curing circumstance, chemical composition of source materials, and casting time. As a result, it was very difficult to obtain a high correlation coefficient in NLMR process.

F_i and $(f_{ck})_{28}$ of AA mortars were normalized by a nominal initial flow F_0 and a nominal compressive strength f_0, respectively, to control the lower bound for the initial flow and to improve the performance of the NLMR. The nominal values of F_0 and f_0 were assumed to be 100 mm (3.94 in.), which corresponds to the bottom diameter of cone for flow test, and 10 MPa (1450 psi), respectively. Based on NLMR analysis of the database, F_i / F_0, and $(f_c')_{28} / f_0$ of mortars activated by sodium silicate and sodium hydroxide powders can be expressed as below;

$$\frac{F_i}{F_0} = 6.5\left[\frac{Q_A{}^{0.05} \times (S_A / S_{A0})^{0.3} \times (1 + S/B)^{0.5}}{(W/B)^{1.5}}\right]^{-0.85} \geq 1 \quad (5)$$

$$\frac{(f_c')_{28}}{f_{co}} = 148\left[\frac{Q_A \times (S_A / S_{A0} + k_1)^{0.3}}{(W/B)}\right]^{1.23} \quad (6)$$

where $k_1 = (S/B)^{0.5}$ for $S/B \leq 2.5$ and $(S/B)^{-0.5}$ for $S/B > 2.5$.

In addition, the two parameters A_1 and B_1 of Eq. (1) to predict the compressive strength development of GGBS-based AA mortars were predicted by NLMR analysis of the database as follows:

$$A_1 = 0.39\left[\frac{(W/B)^2 \times (1 + k_1)^{0.3}}{Q_A \times (S_A / S_{A0})^{0.1}}\right]^{0.66} \quad (7)$$

$$B_1 = 1.1\left[\frac{(W/B)^2 \times (1 + k_1)^{0.3}}{Q_A \times (S_A / S_{A0})^{0.1}}\right]^{-0.09} \quad (8)$$

A_1 and B_1 obtained from Eqs. (7) and (8) against W/B and S/B are presented in Fig. 4. The prediction obtained for B_1 is closer to the experimental results than that for A_1.

COMPARISONS WITH TEST RESULTS

Comparisons of test results and predictions obtained from the proposed simplified equations (5 to 8) and 4×8×4×1 networks are shown in Fig. 6: Fig. 6 (a) for F_i and Fig. 6 (b) for $\left(f_c^{'}\right)_{28}$. The mean γ_m and standard deviation γ_s of ratios between measured and predicted F_i are 1.0 and 0.15, respectively, for equations based on NLMR analysis and 0.99 and 0.05, respectively, for 4×8×4×1 NN. In addition, γ_m and γ_s of ratios between measured and predicted $\left(f_c^{'}\right)_{28}$ are 1.06 and 0.26, respectively, for equations and 1.0 and 0.24, respectively, for 4×8×4×1 NN. The developed 4×8×4×1 NNs better predict the values of F_i and $\left(f_c^{'}\right)_{28}$ of mortars activated by sodium silicate and sodium hydroxide powders than the simplified equations developed from NLMR analysis. However, predictions obtained from simplified equations also show good agreement with test results.

Table 5 gives comparisons between measured and predicted compressive strengths using Eq. (1) at different age of GGBS-based mortars activated by sodium silicate and sodium hydroxide powders. Values of $\left(f_c^{'}\right)_{28}$, A_1 and B_1 required by Eq. (1) are obtained from Eqs. (6) to (8). The proposed equations well describe the compressive strength development of GGBS-based AA mortars according to age, though they slightly overestimate the early strength.

CONCLUSIONS

Thirty six ground granulated blast-furnace slag (GGBS) and eighteen fly ash (FA) based mortars activated by sodium silicate and sodium hydroxide powders were mixed and tested. The main

variables investigated were Na_2O-to-source material ratio, water-to-binder ratio, and fine aggregate-to-binder ratio. Multi-layered feed-forward neural network models were built to evaluate the initial flow and 28-day compressive strength of alkali-activated (AA) mortars. In addition, simplified equations based on nonlinear multiple regression analysis were proposed and compared with test results and neural network model developed. The following conclusions may be drawn from the experimental and analytical investigations of this study:

1. The flow of AA mortars tested increased with the increase of water-to-binder ratio and decrease of fine aggregate-to-binder ratio. When the fine aggregate-to-binder ratio was larger than 2.5, the flow of AA mortars sharply decreased.
2. Much higher compressive strength developed in GGBS-based AA mortars than in FA-based AA mortars that developed insignificant strength.
3. The 28-day compressive strength of GGBS-based mortars activated by the combination of sodium silicate and sodium hydroxide was generally lower than that of GGBS-based mortars activated by sodium silicate only for the same value of Na_2O-to-source material ratio.
4. The 28-day compressive strength of AA mortars commonly decreased with the increase of water-to-binder ratio. The decreasing rate was more prominent in AA mortars with Na_2O-to-source material ratio of 0.089 than 0.039.
5. The compressive strength of GGBS-based AA mortars increased with the increase of fine aggregate-to-source material ratio up to a ratio of 2.5 beyond which it dramatically decreased, regardless of Na_2O-to-source material ratio.

6. The developed neural networks better predicted the initial flow and 28-day compressive strength of mortars activated by sodium silicate and sodium hydroxide powders than the proposed simplified equations. However, predictions obtained from simplified equations showed good agreement with test results.
7. The compressive strength development of GGBS-based AA mortars was reasonably evaluated by the formula specified in ACI 209 with the calibrated parameters obtained from the current regression analysis, though their early strength was slightly overestimated.

ACKNOWLEDGMENTS

This work was supported by the National Research Institute of Cultural Heritage and the Regional Research Centers Program (Bio-housing Research Institute), granted by the Korean Ministry of Education & Human Resources Development. The authors wish to express their gratitude for financial support.

REFERENCES

1. Wang, S. D., Pu, X. C., Scrivener, K. L., and Pratt, P. L., “Alkali-Activated Slag Cement and Concrete: A Review of Properties and Problems,” Advances in Cement Research, V. 7, No. 27, 1995, pp. 93-102.

2. Pacheco-Torgal, F., Castro-Gomes, J., and Jalali, S., "Alkali-Activated Binders: A Review. Part 2. About Materials and Binder Manufacture," Construction and Building Materials, V. 22, No. 7, 2008, pp. 1305-1314.

3. Roy, D. M., "Alkali-Activated Cements: Opportunities and Challenges," Cement and Concrete Research, V. 29, 1999, pp. 249-254.

4. Duxson, P., Provis, J. L., Lukey, G. G., and van Deventer, J. S. J., "The Role of Inorganic Polymer Technology in the Development of 'Green Concrete'," Cement and Concrete Research, V. 37, No. 12, 2007, pp. 1590-1597.

5. Gartner, E., "Industrially Interesting Approaches to "Low-CO_2" Cements," Cement and Concrete Research, V. 34, No. 9, 2004, pp. 1489-1498.

6. Wang, S. D., Scrivener, K. L., and Pratt, P. L., "Factors Affecting the Strength of Alkali-Activated Slag," Cement and Concrete Research, V. 24, 1994, pp. 1033-1043.

7. Palomo, A., Grutzeck, M. W., and Blanco, M. T., "Alkali-Activated Fly Ashes: A Cement for the Future," Cement and Concrete Research, V. 29, 1999, pp. 1323-1329.

8. Shi, C., Krivenko, P. V, and Roy, D., Alkali-Activated Cements and Concretes, Taylor and Francis, England, 2006.

9. Duxson, P., Fernández-Jiménez, A., Provis, J. L., Lukey, G. G., Palomo, A., and van Deventer, J. S. J., "Geopolymer Technology: The Current State of the Art," Journal of Materials Science, V. 42, No. 9, 2007, pp. 2917-2933.

10. Khale, D., and Chaudhary, R., “Mechanism of Geopolymerization and Factors Influencing Its Development: A Review,” Journal of Materials Science, V. 42, 2007, pp. 729-746.

11. Shi, C., and Day, R. L., “Comparison of Different Methods for Enhancing Reactivity of Pozzolans,” Cement and Concrete Research, V. 31, 2001, pp. 813-818.

12. Brough, A. R., and Atkinson, A., “Sodium Silicate-Based, Alkali-Activated Slag Mortars: Part I. Strength, Hydration and Microstructure,” Cement and Concrete Research, V. 32, 2002, pp. 865-879.

13. Neville, A. M., Properties of Concrete, Longman, England, 1995.

14. Yang, K. H., Song, J. K., Ashour, A. F., and Lee, E. T., “Properties of Cementless Mortar Activated by Sodium Silicate,” Construction and Building Materials, V. 22, No. 8, 2008, pp. 1981-1989.

15. ASTM, Annual Book ASTM Standards, American Society for Testing and Materials (ASTM), Philadelphia, USA, 2003.

16. Yang, K. H., and Song, J. K., “Workability Loss and Compressive Strength Development of Cementless Mortars Activated by Combination of Sodium Silicate and Sodium Hydroxide,” Submitted to Journal of Materials in Civil Engineering, ASCE, for publication, 2007.

17. ACI 209R-92, Prediction of Creep, Shrinkage, and Temperature Effects in Concrete Structures, ACI Manual of Concrete, Practice Part 1, USA, 1994.

18. Kaveh, A., and khalegi, A., “Prediction of Strength for Concrete Specimens using Artificial Neural Networks,” Advances in Computational Structures Technology, B. H. V. Topping, ed., Civil-Comp Press, Edinburgh, U.K., 1998, pp. 165-171.

19. Demuth, H., and Beale, M. Neural network toolbox for user with MATLAB. The Math Works, Inc., USA, 2002.

20. SPSS Inc., SPSS 13.0: Regression Models, Prentice Hall, USA, 2004.

TABLES AND FIGURES

List of Tables:

List of Figures:

Table 1-Mixing details and result summary of AA mortars tested.

Group	Mortar No.	Source material (SM)	Activator		W/B	S/B	Na_2O/SM	Q_A*	F_i (mm)	f_c' (MPa)					
			Type	SiO_2/Na_2O						1 day#	3 days	7 days	28 days	56 days	91 days
I	1	GGBS	Sodium silicate + sodium hydroxide	0.75	0.3	3.0	0.038	0.0117	100.0	12.8	20.5	25.5	26.8	28.7	30.8
	2						0.089	0.0230	100.0	37.9	47.7	62.9	70.1	71.3	72.7
	3				0.4		0.038	0.0117	113.8	11.2	18.2	21.3	24.1	26.9	29.0
	4						0.089	0.0230	111.0	33.3	39.5	48.6	60.7	62.7	64.1
	5				0.5	0.0	0.038	0.0117	280.0	4.6	11.2	14.0	16.5	20.0	23.2
	6					1.5		0.0117	261.0	4.9	11.7	14.5	17.2	20.9	23.5
	7					2.0		0.0117	255.0	4.6	12.8	14.3	18.8	22.9	24.6
	8					2.5		0.0117	235.0	5.2	14.2	14.7	22.6	25.1	27.2
	9					3.0		0.0117	197.4	5.9	13.2	15.8	20.2	23.5	25.1
	10					3.5		0.0117	130.5	5.9	12.1	15.7	18.5	23.4	25.1
	11					0.0	0.089	0.0230	277.0	14.5	23.6	26.9	34.6	39.9	42.3
	12					1.5		0.0230	263.0	15.6	31.2	33.5	39.7	44.8	47.6
	13					2.0		0.0230	252.0	12.5	33.8	36.8	43.7	47.5	49.6
	14					2.5		0.0230	242.5	16.3	30.2	42.1	48.6	51.5	55.9
	15					3.0		0.0230	180.0	16.4	29.2	35.0	43.7	50.6	52.8
	16					3.5		0.0230	124.5	18.2	26.4	28.8	36.7	43.6	47.5
	17				0.6	3.0	0.038	0.0117	247.0	4.2	9.5	11.9	16.5	18.8	20.8
	18						0.089	0.0230	233.0	14.1	18.5	22.4	28.0	33.7	36.8
II	19	FA	Sodium silicate + Sodium hydroxide	0.75	0.3	3.0	0.038	0.0011	105.0	1.2	2.5	4.5	6.0	9.0	11.0
	20						0.089	0.0021	100.0	1.7	3.0	5.2	7.2	12.2	15.2
	21				0.4		0.038	0.0011	125.0	0.9	1.8	2.4	4.0	4.8	5.7
	22						0.089	0.0021	117.0	1.6	1.8	1.6	4.8	7.7	8.9
	23				0.5	0.0	0.038	0.0011	300.0	-	0.3	0.3	0.9	1.2	2.4
	24					1.5		0.0011	277.0	-	0.3	0.3	1.1	1.4	2.4
	25					2.0		0.0011	263.0	-	0.3	0.3	1.3	1.4	2.7
	26					2.5		0.0011	245.5	-	0.3	0.3	1.5	1.7	2.5
	27					3.0		0.0011	210.0	-	1.0	1.3	1.7	1.8	1.8

* Q_A indicates the alkali quality coefficient proposed by Yang et al[9].

Table 1 (continued) -Mixing details and result summary of AA mortars tested.

Group	Mortar No.	Source material (SM)	Activator		W/B	S/B	Na_2O/SM	Q_A*	F_i (mm)	f_c' (MPa)					
			Type	SiO_2/Na_2O						1 day#	3 days	7 days	28 days	56 days	91 days
II	28	FA	Sodium silicate + Sodium hydroxide	0.75	0.5	3.5	0.038	0.0011	135.5	-	0.2	0.3	1.3	1.8	2.3
	29					0.0	0.089	0.0021	300.0	-	0.2	0.6	1.2	2.9	3.0
	30					1.5		0.0021	275.0	-	0.2	0.4	1.5	1.7	2.5
	31					2.0		0.0021	269.0	-	0.2	0.4	1.9	2.2	3.4
	32					2.5		0.0021	246.0	-	0.2	0.5	2.2	2.5	3.8
	33					3.0		0.0021	197.0	-	0.2	1.0	2.5	2.9	4.0
	34					3.5		0.0021	145.0	-	0.2	0.4	1.9	2.4	3.4
	35				0.6	3.0	0.038	0.0011	260.0	-	0.1	0.3	0.6	0.9	1.2
	36						0.089	0.0021	250.0	-	0.2	0.7	1.2	1.8	2.5
III	37	GGBS	Sodium silicate	0.9	0.3	3.0	0.038	0.0131	100.0	15.1	21.7	25.0	28.5	30.6	34.5
	38						0.089	0.0245	100.0	39.8	49.3	64.5	71.6	73.8	74.0
	39				0.4		0.038	0.0131	122.5	11.9	19.9	21.8	26.2	31.4	33.2
	40						0.089	0.0245	120.0	34.9	41.5	50.4	62.8	64.9	65.7
	41				0.5	0.0	0.038	0.0131	285.0	6.0	11.6	16.1	20.0	23.2	25.3
	42					1.5		0.0131	263.0	6.2	13.8	19.8	24.9	27.8	30.5
	43					2.0		0.0131	254.0	7.2	14.4	20.1	26.3	28.6	31.7
	44					2.5		0.0131	237.0	7.1	15.1	22.1	28.3	30.5	33.5
	45					3.0		0.0131	186.0	6.7	12.9	17.9	21.7	24.7	26.2
	46					3.5		0.0131	131.0	6.1	11.3	15.4	20.4	22.5	24.9
	47					0.0	0.089	0.0245	280.0	14.1	30.4	42.5	50.9	54.9	57.9
	48					1.5		0.0245	262.0	17.3	33.1	44.0	55.5	58.8	60.3
	49					2.0		0.0245	250.0	18.6	35.4	46.0	59.3	61.8	63.3
	50					2.5		0.0245	232.0	18.4	34.4	48.1	61.1	62.8	65.5
	51					3.0		0.0245	172.0	18.5	32.6	45.7	53.9	56.2	58.3
	52					3.5		0.0245	130.0	17.1	32.2	38.4	50.6	53.7	54.9
	53				0.6	3.0	0.038	0.0131	250.0	4.2	10.3	13.7	17.2	19.9	21.5
	54					3.0	0.089	0.0245	247.5	14.4	23.0	30.8	37.9	43.5	45.5

Testing compressive strength of FA-based AA mortars at age of one day failed as specimens were in plastic state.
* Q_A indicates the alkali quality coefficient proposed by Yang et al[9].

1 MPa = 145 psi; 1 mm = 0.039 in.

Table 2 - Chemical composition of the selected source materials (% by mass).

Materials	SiO_2	Al_2O_3	Fe_2O_3	CaO	MgO	K_2O	Na_2O	TiO_2	SO_3	LOI*
FA	57.70	28.60	5.08	4.70	0.67	0.57	0.37	1.53	0.68	0.1
GGBS	34.70	13.80	0.11	44.60	4.38	0.48	-	0.74	0.95	0.24
* Loss on ignition.										

Table 3-Range of input variables in the database used to generalize the neural network.

Input variables*		Total data		Training subset		Validation subset		Test subset	
		min	max	min	max	min	max	min	max
Na_2O/SM	FA	0.0227	0.164	0.0227	0.164	0.0379	0.139	0.0269	0.114
	GGBS	0.0227	0.139	0.0227	0.139	0.0269	0.1138	0.0269	0.089
Q_A	FA	0.0001	0.0056	0.0001	0.0056	0.0011	0.0054	0.0011	0.0054
	GGBS	0.0103	0.0361	0.0103	0.0361	0.0117	0.0352	0.0117	0.0325
$S_A/(S_A)_0$	FA	0.847	0.847	0.847	0.847	0.847	0.847	0.847	0.847
	GGBS	1.051	2.04	1.051	2.04	1.501	1.537	1.501	2.04
W/B	FA	0.3	0.6	0.3	0.6	0.4	0.6	0.4	0.6
	GGBS	0.3	0.6	0.3	0.6	0.3	0.6	0.4	0.6
S/B	FA	0	3.5	0	3.5	0	3.0	1.5	3.0
	GGBS	0	3.5	0	3.5	0	3.0	2.0	3.5
Note : * In the input layer of network A, FA and GGBS were identified as numerals 1 and 2, respectively, and the use of sodium silicate only and the combination of sodium silicate and hydroxide silicate were also identified as numerals 1 and 2, respectively.									

Table 4 -Comparison of outputs and targets for different network structures.

Network structures*		Mean (γ_m)		Standard deviation(γ_s)		Coefficient of determination (R^2)	
		F_i	$(f_c')_{28}$	F_i	$(f_c')_{28}$	F_i	$(f_c')_{28}$
Network A	6×12×1	1.02	1.02	0.12	0.28	0.95	0.96
	6×12×6×1	1.0	1.04	0.094	0.29	0.97	0.96
	6×12×6×6×1	1.02	1.1	0.11	0.31	0.95	0.95
Network B	4×8×1	1.01	1.01	0.1	0.28	0.96	0.96
	4×8×4×1	1.0	0.99	0.1	0.27	0.96	0.96
	4×8×4×4×1	1.02	1.02	0.11	0.32	0.94	0.94
* The first and the last numbers indicate the numbers of neurons in input and output layers, respectively, and the others refer to the number of neurons in hidden layers.							

Table 5 –Statistical comparisons of predicted strength of GGBS-based AA mortars with age.

Statistical values	$(f_c')_{Exp.}/(f_c')_{Pre}$					
	1 day	3 days	7 days	28 days	56 days	91 days
γ_m	1.11	1.10	0.99	1.02	1.04	1.07
γ_s	0.17	0.16	0.14	0.15	0.14	0.14

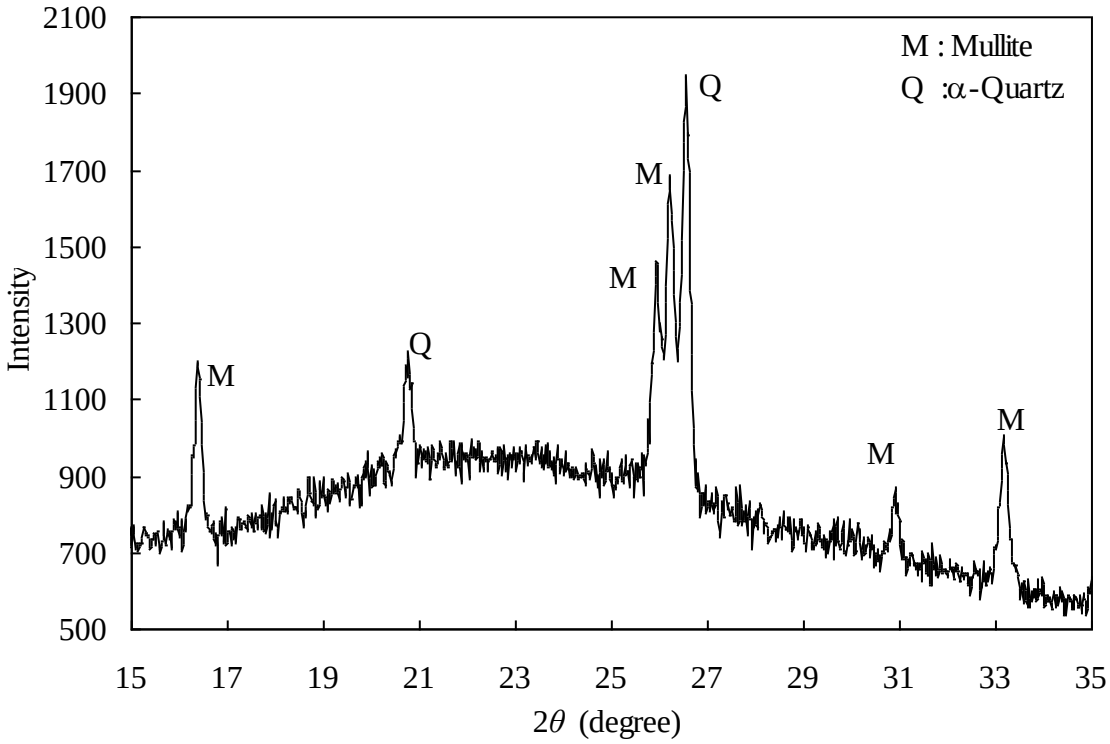

(a) Fly ash

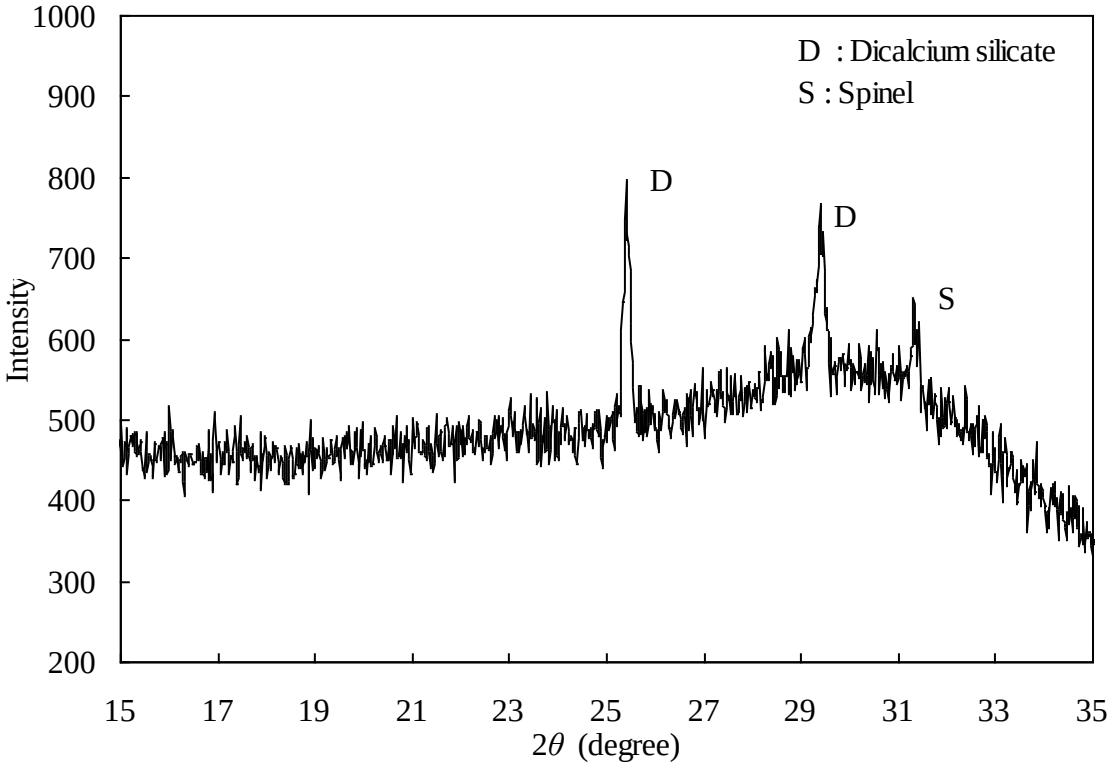

(b) Ground granulated blast-furnace slag

Fig. 1 – XRD patterns of source materials used.

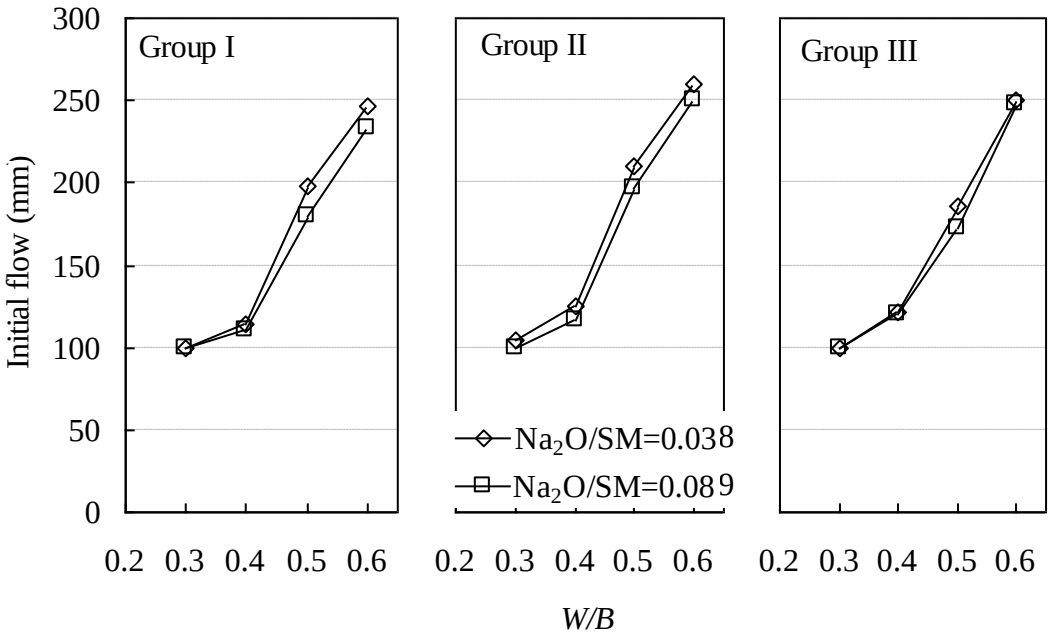

(a) Effect of W/B ratio (S/B=3.0)

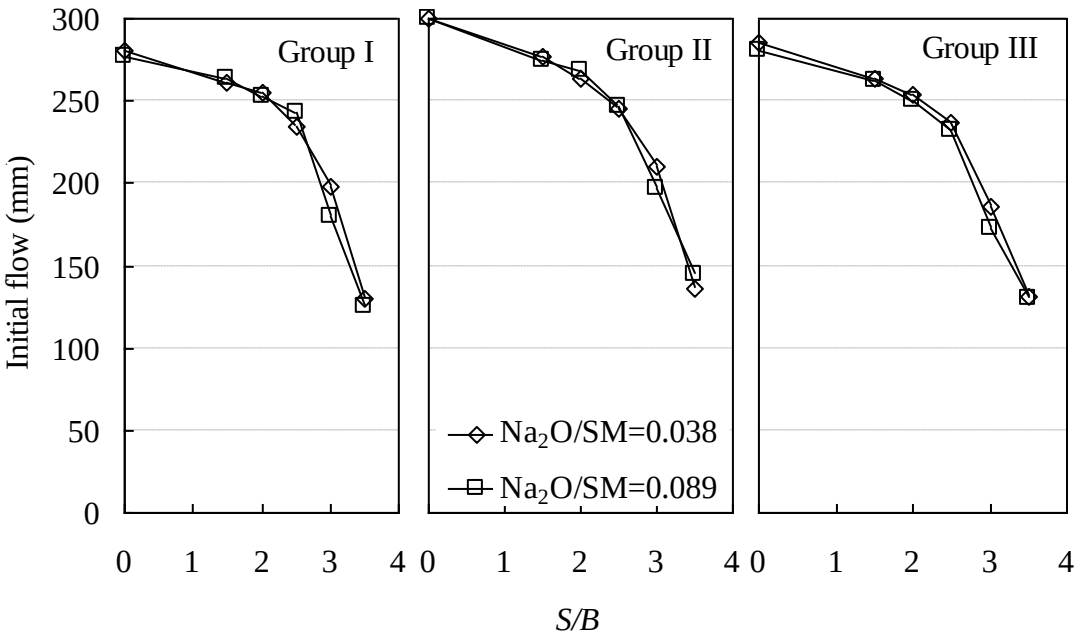

(b) Effect of S/B ratio (W/B=0.5)

Fig. 2 – Initial flow of AA mortars studied. (1 mm = 0.039 in.)

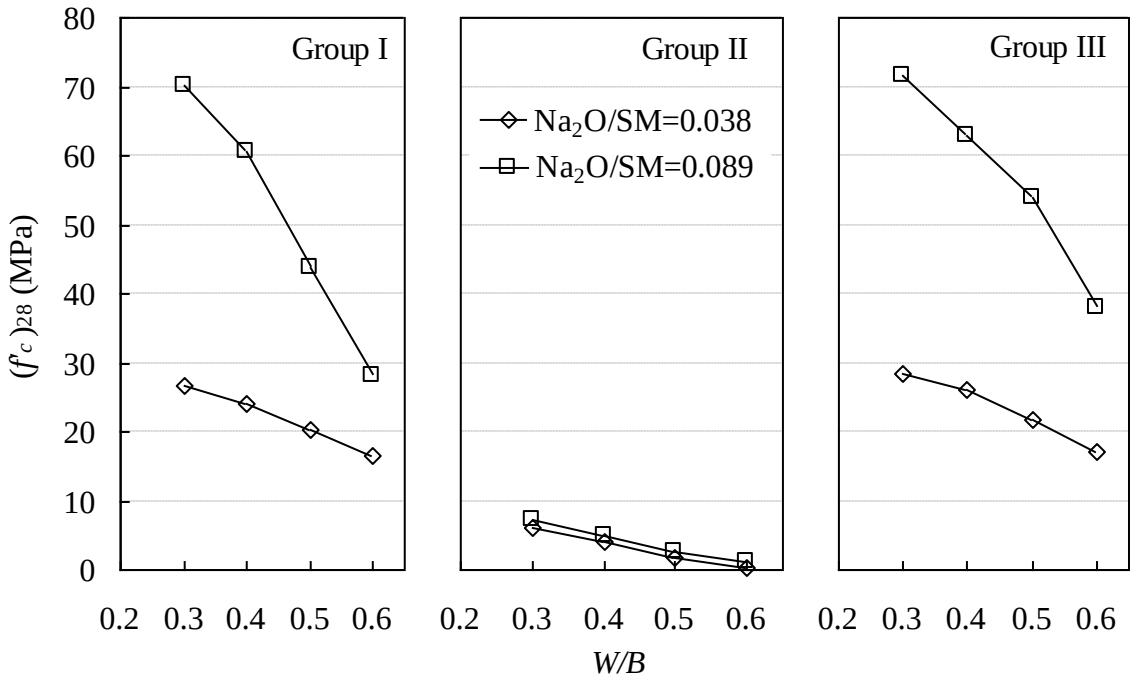

(a) Effect of W/B ratio (S/B=3.0)

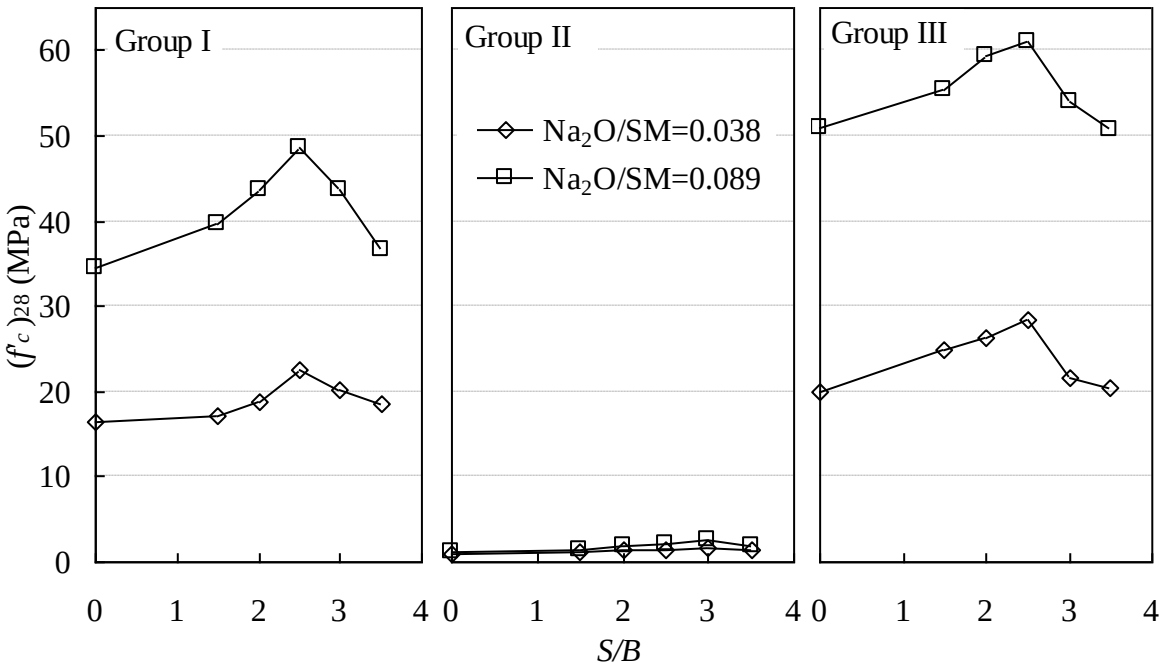

(b) Effect of S/B ratio (W/B=0.5)

Fig. 3 – 28-day compressive strength of AA mortars studied. (1 MPa = 145 psi)

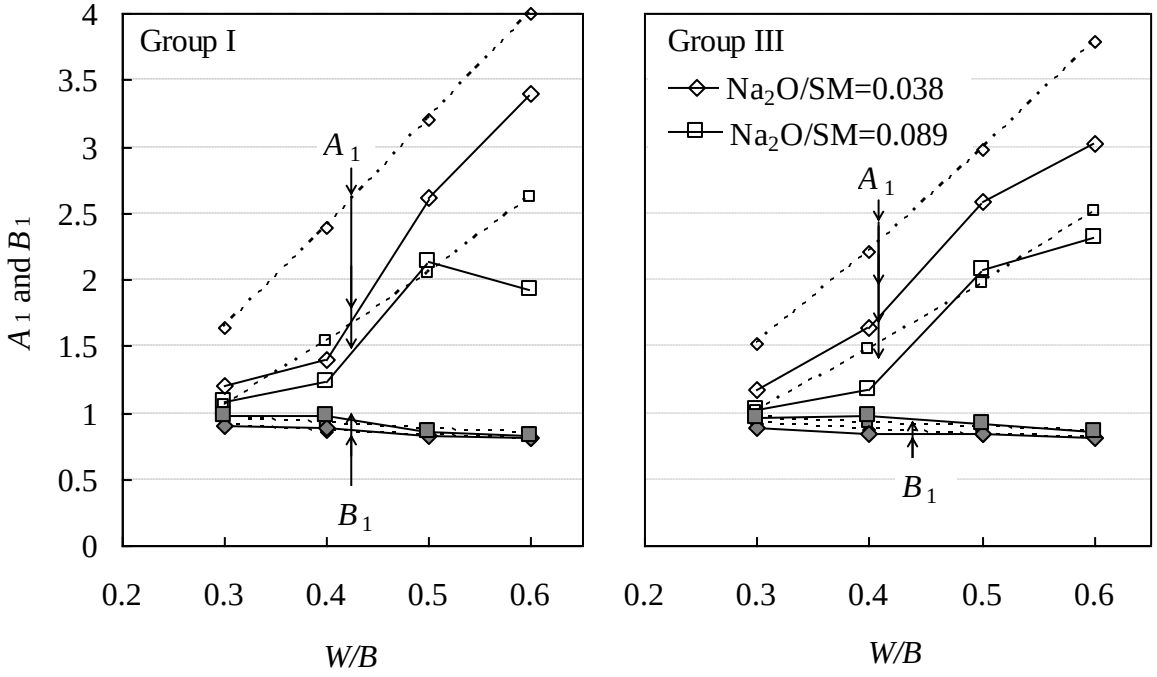

(a) Effect of W/B ratio (S/B=3.0)

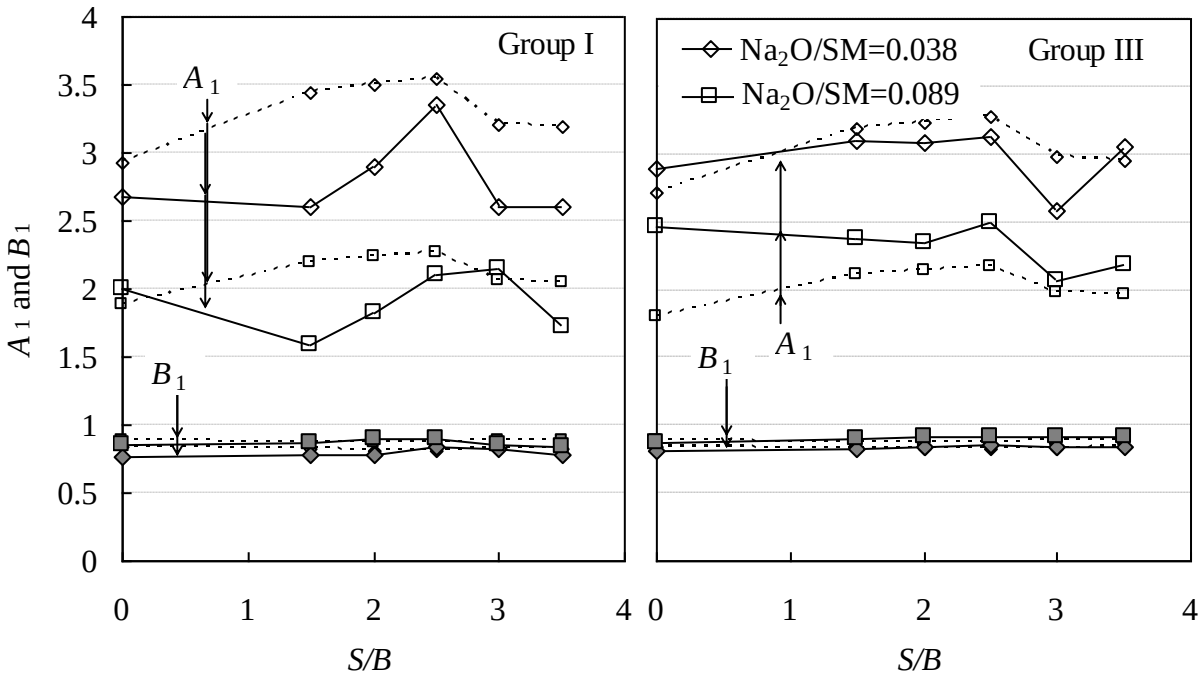

(b) Effect of S/B ratio (W/B=0.5)

Fig. 4 – Variation of parameters A_1 and B_1 for GGBS-based AA mortars.

(Solid and dotted lines refer to values obtained from the test results, and Eqs. (7) and (8), respectively)

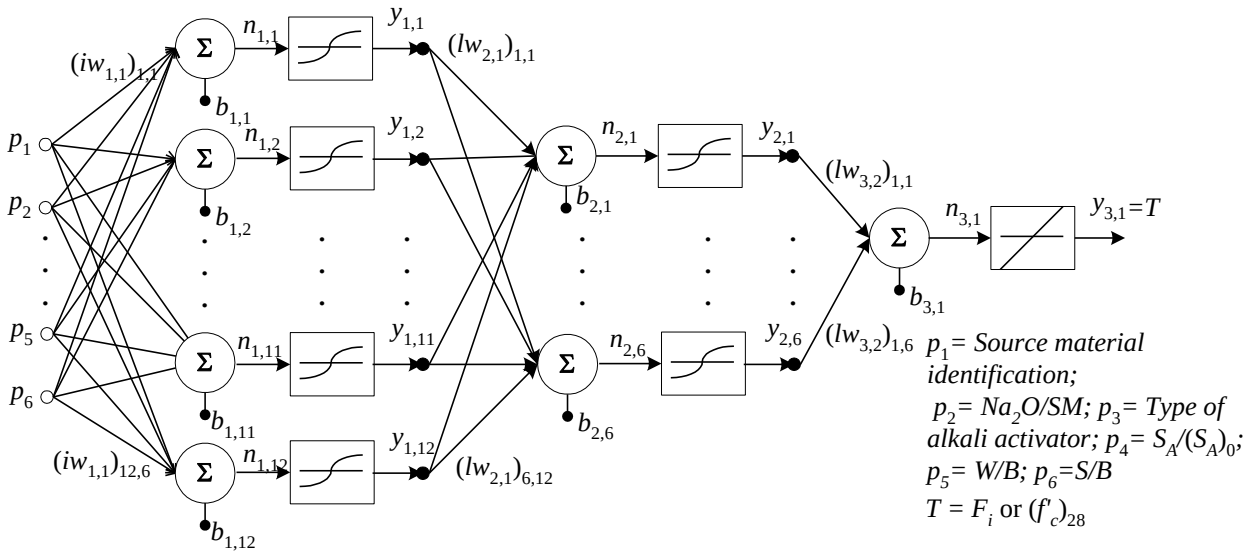

(a) 6×12×6×1 network

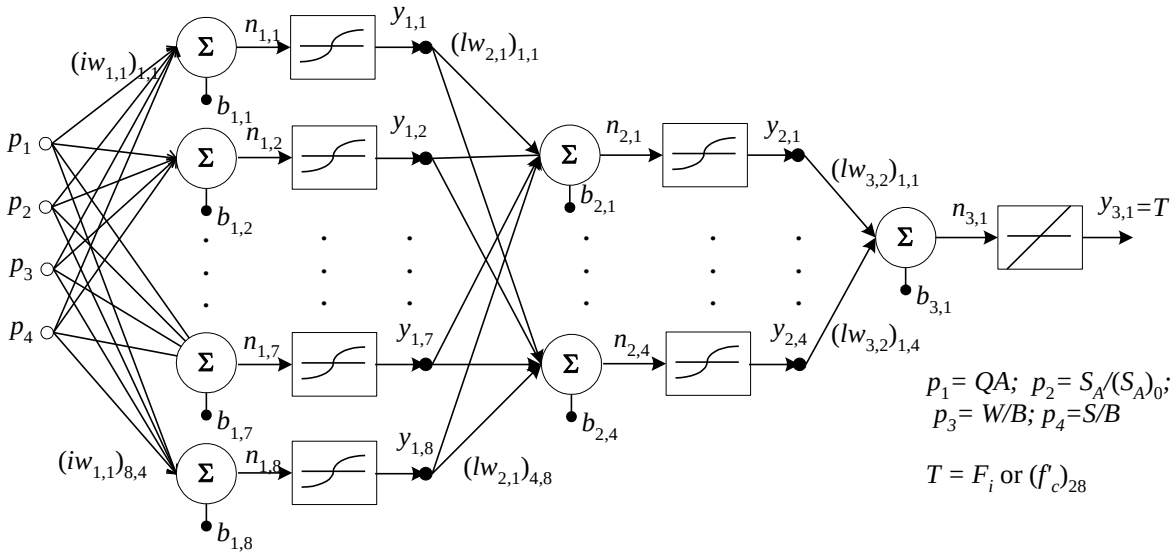

(b) 4×8×4×1 network

Fig. 5- Architecture of networks for AAS mortars.

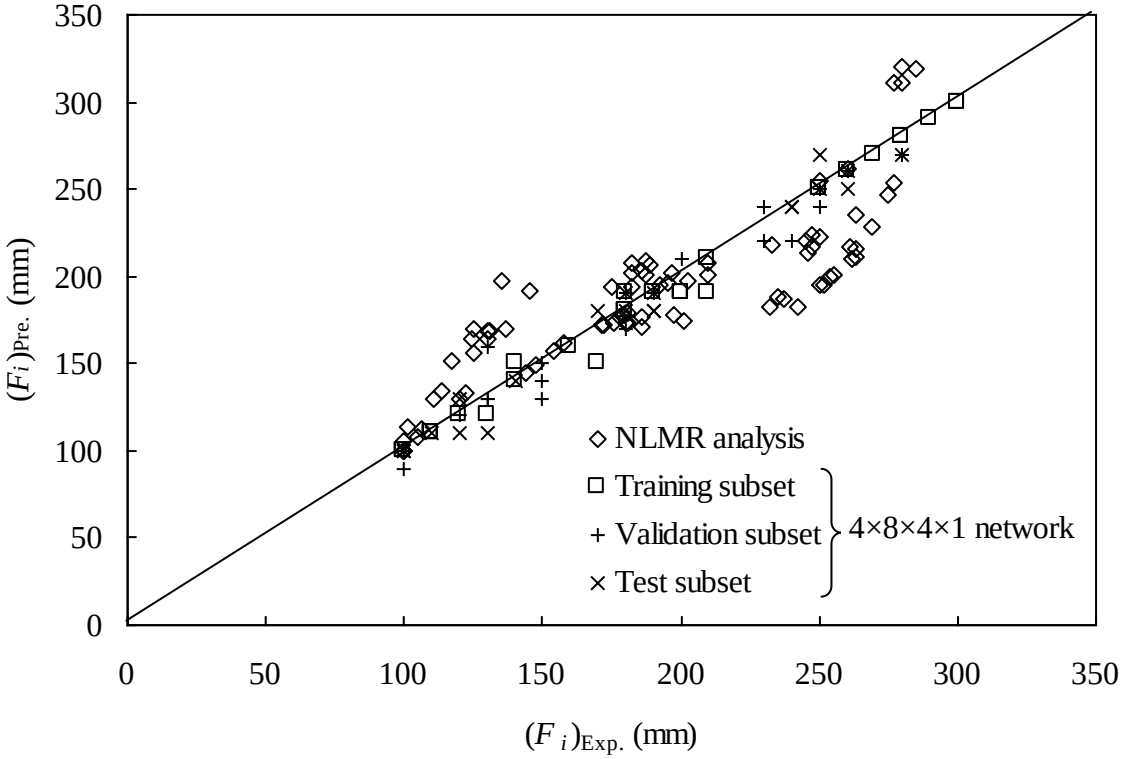

(a) Initial flow F_i

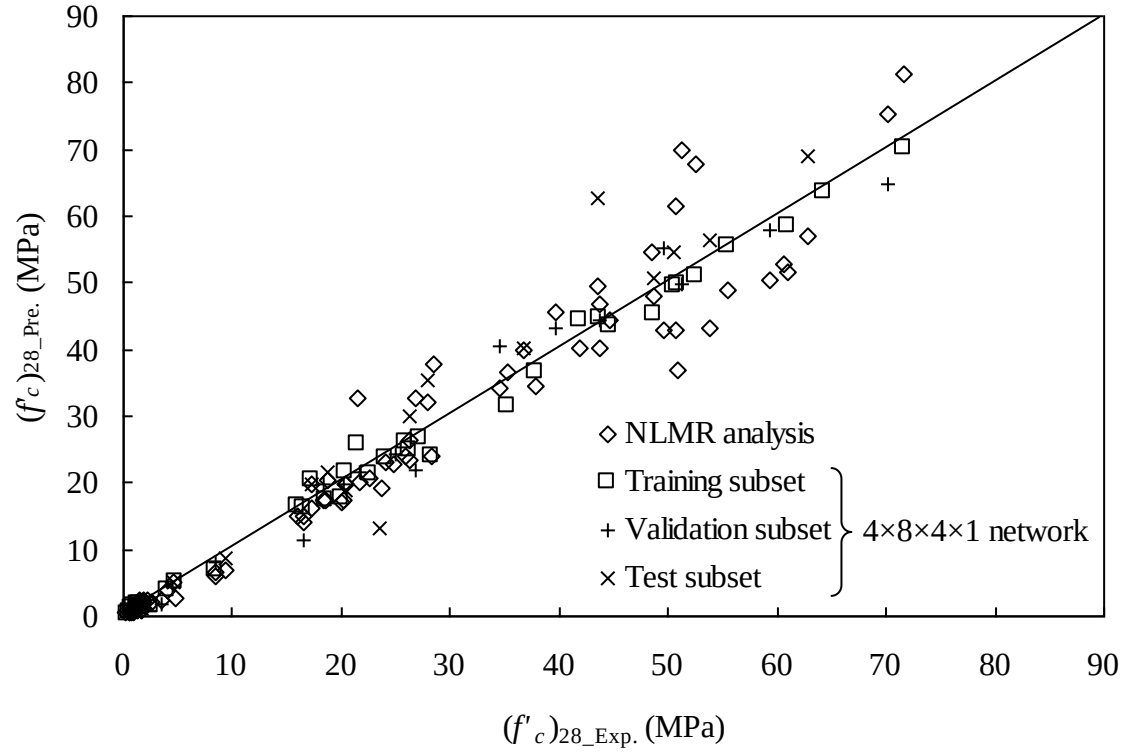

(b) 28-day compressive strength $\left(f_c^{'}\right)$

Fig. 6- Comparisons of predictions and experimental results. (1 mm = 0.039 in.; 1 MPa = 145 psi)